



# HHS Public Access

Author manuscript

*Nanomedicine*. Author manuscript; available in PMC 2019 February 01.

Published in final edited form as:

*Nanomedicine*. 2018 February ; 14(2): 397–404. doi:10.1016/j.nano.2017.10.004.

## Challenges and opportunities in developing targeted molecular imaging to determine inner ear defects of sensorineural hearing loss

Mohammad N. Kayyali, M.D.<sup>a</sup>, Alexander C. Wright, Ph.D.<sup>b</sup>, Andrew J. Ramsey, Ph.D.<sup>a</sup>, Jason A. Brant, M.D.<sup>a</sup>, Joel M. Stein, M.D., Ph.D.<sup>b</sup>, Bert W. O'Malley Jr, M.D.<sup>a</sup>, and Daqing Li, M.D.<sup>\*,a</sup>

<sup>a</sup>Department of Otorhinolaryngology- Head & Neck Surgery, University of Pennsylvania School of Medicine, Philadelphia, Pennsylvania

<sup>b</sup>Department of Radiology, University of Pennsylvania, Philadelphia, Pennsylvania

### Abstract

The development of inner ear gene carriers and delivery systems has enabled genetic defects to be repaired and hearing to be restored in mouse models. Today, promising advances in translational therapies provide confidence that targeted molecular therapy for inner ear diseases will be developed. Unfortunately, the currently available non-invasive modalities, such as Computerized Tomography scan or Magnetic Resonance Imaging provide insufficient resolution to identify most pathologies of the human inner ear, even when the current generation of contrast agents is utilized. The development of targeted contrast agents may play a critical role in determining the cause of, and treatment for, sensorineural hearing loss. Such agents should be able to pass through the cochlea barriers, possess minimal cytotoxicity, easily conjugate to a targeting agent and without distorting the anatomic details. This review focuses on a series of contrast agents which may fit these criteria for potential clinical application.

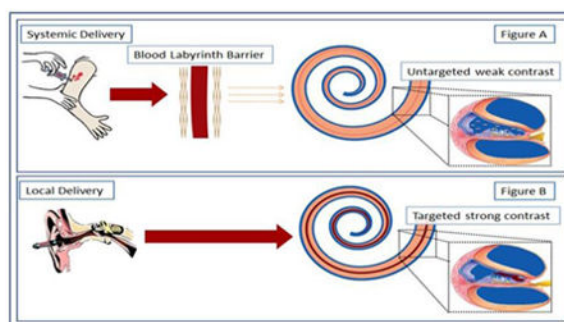
### Graphical abstract

---

\*Corresponding Author: Daqing Li, M.D., Address: Department of Otorhinolaryngology- Head & Neck Surgery, University of Pennsylvania Health System, 1212 BRB, 421 Curie Blvd, Philadelphia, PA 19104, Tel: 1-215-615-0854, Fax: 1-215-573-1934, lidaqing@pennmedicine.upenn.edu.

There are no conflicts of interest.

**Publisher's Disclaimer:** This is a PDF file of an unedited manuscript that has been accepted for publication. As a service to our customers we are providing this early version of the manuscript. The manuscript will undergo copyediting, typesetting, and review of the resulting proof before it is published in its final citable form. Please note that during the production process errors may be discovered which could affect the content, and all legal disclaimers that apply to the journal pertain.



## Keywords

Molecular imaging; targeted nano particles; inner ear imaging

## Introduction

It is estimated that 48 million people, or 20.3% of the American population, 12 years or older suffered from either bilateral or unilateral hearing loss between 2001 and 2008<sup>1</sup>. There are numerous etiologies of hearing loss both congenital and acquired. More than 50% of the cases of congenital hearing loss stem from genetic causes, with more than 50 associated genes already identified<sup>2,3</sup>. Later in life, acquired hearing loss due to environmental exposures and ageing are significant problems. A majority of Americans over 70 suffer from bilateral hearing loss<sup>1</sup>. There is a wide range of inner ear pathologies that can cause sensorineural hearing loss ; ranging from gross congenital malformations of the inner ear<sup>4</sup>, to loss of hair cells<sup>5</sup>, to mutations in key proteins such as myosin VIIa<sup>2,6</sup>. Detection of these different types of pathologies presents widely differing diagnostic challenges. Although audiologic evaluation can accurately quantify the loss of hearing, it provides minimal information about the underlying pathology. Additionally, modalities commonly utilized for diagnosis in other anatomic sites such as tissue biopsy are not an option for the inner ear as any violation of this sensitive area would carry an unacceptable risk of complete auditory and vestibular loss. Consequently, there is a need for reliable, non-invasive techniques that can determine the etiology of sensorineural hearing loss. Imaging techniques such as magnetic resonance imaging (MRI) and X-ray based computed tomography (CT) have become routine in clinical settings, including otorhinolaryngology. CT can provide high resolution of osseous structures including those of the temporal bone but lacks fine discrimination of soft tissue structures<sup>7,8</sup>. MRI is extremely useful in imaging soft tissues<sup>9</sup> but its use in the inner ear can be limited due to artifacts arising from the air-bone interface encountered in the pneumatized temporal bone and it lacks definition of the fine bony structures of the ear. CT and MRI play complementary roles in identifying cases of hearing loss due to congenital or acquired structural abnormalities, neoplasm, infection and inflammation.

Clinical MRI and CT imaging can detect macroscopic changes in morphology such as cochleovestibular malformations or enlarged vestibular aqueduct<sup>4,10,11</sup>. However, the underlying pathologies for a majority of causes of sensorineural hearing loss manifest on a

microscopic or molecular scale which currently are only detectable by histological techniques that are of limited clinical use. For instance, the mutation of key proteins such as connexin 26 may lead to patients possessing apparently normal inner ear morphology, but still suffering from significant hearing loss<sup>12</sup>. Additionally, the loss of inner ear hair cell function is a common cause of hearing loss. Hair cell damage can result from a variety of processes; from elevated levels of reactive oxygen species resulting from exposure to noise<sup>5</sup>, to a range of mutations in key proteins such as myosin VIIa<sup>6</sup>. Currently, neither CT nor MRI has sufficient resolution to detect morphological changes within the cochlea such as loss of hair cells, much less changes on a molecular level. New imaging modalities or new techniques utilizing existing modalities will be required to determine the causes of hearing loss at the molecular level. The sensitivity and specificity of both MR and CT imaging to detect various pathological processes are enhanced by the use of contrast agents<sup>13, 14</sup>. Conventional contrast agents differentially increase or decrease the signal in tissues of interest and generally rely on vascular changes such as those induced by inflammation or malignancy. Imaging specificity can be further increased by using contrast agents designed to target particular molecular biomarkers<sup>15, 16</sup>. This results in the clustering of the contrast agents around the targeted molecule which enhances the image's contrast to noise ratio and may reduce the amount of agent that is required<sup>13</sup>. Contrast agents are administered intravenously for most clinical applications, but systemic delivery to the inner ear can be impeded by the blood labyrinth barrier<sup>17</sup>. The ease with which an agent penetrates this barrier is dependent on various properties. It is also possible to introduce an agent into the inner ear using an intratympanic injection<sup>18, 19</sup>, although the suitability of this method may be dependent on the ability of the contrast agent to pass through the round window membrane.

## The Suitability of Contrast agents for Targeting: an Overview

### MRI contrast agents

**Gadolinium Contrast agents**—Gadolinium compounds are the most widely used class of MRI contrast agents. The paramagnetic effect of gadolinium results in increased signal intensity on T1-weighted MR images. The current generation of gadolinium agents is designed to maximize the sensitivity of MR imaging while being highly water soluble and minimizing toxicity<sup>13, 16, 20, 21</sup>. Multiple targeted gadolinium compounds have been developed. For example, a complex synthesis was used to produce a construct that consisted of a gadolinium agent conjugated to a collagen-specific peptide<sup>22</sup>. This construct was then used to target myocardial scars<sup>22</sup>, enabling high contrast images of scar tissue to be produced<sup>22</sup>.

Gadolinium contrast agent, has been encased in glycol chitosan<sup>23</sup> and liposomes<sup>24, 25</sup> in order to reduce the agents' potential toxicity and to simplify their conjugation to targeting compounds. Subsequent studies indicated that both forms of targeted coated constructs possessed minimal cytotoxicity<sup>23, 25</sup>. *In vivo* studies indicated that the liposome encasement allowed for passage through the blood brain barrier<sup>24, 25</sup>. This was exemplified by one construct designed bind to amyloid deposits that produced a large increase in MRI signal intensity in the brain<sup>24</sup>. A second construct identified numerous small intracranial cancerous

masses that were a few millimeters away from the main tumor. These secondary tumors were too small to be detected using non-targeted MRI contrast agents<sup>25</sup>.

Despite a long history of clinical use, there are concerns regarding the potential toxicity of gadolinium contrast agents. The risk of nephrogenic systemic fibrosis related to tissue deposition of gadolinium in patients with impaired renal function is now well known<sup>26</sup>, though it may be ameliorated by improved chelation in newer macrocyclic contrast agents<sup>13</sup>. Gadolinium has also been shown to accumulate in the brain, principally in the dentate nucleus<sup>27-29</sup>, in patients undergoing repeated contrast administration even without renal impairment, although the significance of this finding is unclear<sup>30, 31</sup>. Encapsulating and targeting gadolinium agents may reduce toxicity and the overall gadolinium dose. Local administration may also be an option for inner ear imaging. In any case, the biodistribution and clearance of targeted gadolinium compounds will have to be carefully evaluated.

The utility of current untargeted gadolinium based contrast agents is evidenced by their wide clinical use. However, research studies have demonstrated that it is also possible to produce liposomes containing gadolinium contrast agents that can be targeted to areas of interest. Targeted liposomes can pass through the blood brain barrier and can detect objects that are too small to be visualized by non-targeted agents. These two properties are important in inner ear imaging, due to the presence of the blood labyrinth barrier and the small size of many of the inner ear structures. Although labelling gadolinium is not as straightforward as some of the alternatives, and there are lingering questions about their cytotoxicity, targeted gadolinium compounds are still potentially excellent candidates to be used in the imaging of the inner ear. Gadolinium-based agents can also provide contrast for CT. In clinical practice these compounds are generally only used with CT when the use of an iodine agent is inadvisable<sup>32</sup>, as in cases of severe allergy to an iodine agent<sup>33</sup>. However, a targeted gadolinium contrast agent could be used in CT imaging of the inner ear.

**Superparamagnetic Iron Oxide Nanoparticles (SPIONs)**—SPION and (ultrasmall) USPIO agents consist of nonstoichiometric microcrystalline magnetite cores usually coated with amphiphilic molecules, such as dextran, to provide solubility, decrease aggregation, and allow for biocompatibility<sup>34</sup>. SPIONs develop strong internal magnetization when exposed to a magnetic field. For MRI, this causes a local perturbation in the magnetic field wherever the particles accumulate, manifesting as a decrease in signal on T2 and particularly T2\* or susceptibility-weighted imaging<sup>35, 36</sup>.

Multiple SPION agents have been developed and tested for clinical applications, including imaging liver lesions<sup>37</sup>, lymph nodes<sup>38</sup>, and angiography<sup>39</sup>. Two SPION-based contrast agents, Feridex and Gastromark, received FDA approval in 1996 and additional agents have been approved in Europe<sup>40</sup>. However, iron oxide imaging agents have generally either been halted in development or removed from the market due to poor sales, as they proved inferior to routine contrast agents in the context of improving MRI and CT technology<sup>40, 41</sup>.

Although their clinical applications have been limited, SPION agents have shown greater promise in research fields where the ability to conjugate ligands to these particles has been utilized in numerous applications. The conjugation process is relatively straight forward

using variations of NHS/EDC (N-Hydroxysuccinimide/ ethyl(dimethylaminopropyl) carbodiimide) methodology<sup>42, 43</sup>. Limited cytotoxicity has been detected with uncoated SPIONs<sup>44</sup>. However, MTT (3-(4,5-Dimethylthiazol-2-Yl)-2,5-Diphenyltetrazolium Bromide) studies have indicated that coating untargeted SPIONs with polyvinyl alcohol can almost eliminate cytotoxicity<sup>44</sup>. One study with particles targeted to HeLa tumors showed significant decrease in tumor signal intensity indicative of nanoparticle accumulation, and also demonstrated minimal cytotoxicity<sup>42</sup>. A second construct, was able to pass through the blood brain barrier, doubling the number of Alzheimer's disease plaques detected by MR imaging<sup>43</sup>.

Thus, the ease of conjugation, low toxicity, and prior clinical use of SPIONs make these agents attractive candidates. However, the negative contrast (i.e. decreased signal) produced by SPIONs is generally less desirable than the positive contrast achieved with gadolinium agents. This is particularly true for structures within the pneumatized temporal bone due to already low signal across MR sequences. Additionally, even the fluid-filled inner ear, which is bright on T2-weighted images, can be affected by susceptibility induced signal voids from air-bone interfaces.<sup>45, 46</sup>

### CT contrast agents

**Iodine compounds**—Iodine based contrast agents are inexpensive and are widely used as CT contrast agents<sup>7</sup>. This class of agent usually contains multi-iodinated aromatic groups<sup>14</sup> at its core. Modern iodine contrast agents have been designed to minimize both toxicity and non-specific binding<sup>14</sup>. The use of iodinated compounds as contrast agents takes advantage of the K edge effect<sup>15</sup>. The energy of X-rays produced by clinical CT scanners is set to be similar to the binding energy of the iodine agent's K(1) shell electrons, resulting in greater X-ray attenuation, and increased density or brightness being observed in the CT image<sup>15</sup>.

These agents are generally well tolerated by patients. However, care must be taken to avoid contrast agent induced acute renal toxicity<sup>47</sup>, which can occur in patients with impaired renal function and other risk factors. Additionally, a strong allergic reaction to iodine contrast agents develops in a small number of patients<sup>33</sup>. Conjugating iodine agents to targeting ligands has proven challenging. Additionally, their small size leads to rapid clearance from the blood<sup>48</sup> which limits the amount of time available to accumulate at target sites.

Some progress in overcoming these obstacles has been made by incorporating iodine agents into carrier molecules. For example, iodine contrast agents have been incorporated into liposomes<sup>49</sup>, facilitating greater density, conjugation, and longer circulation times. CT imaging with targeted liposomes containing an iodine contrast agent have been used to detect activated endothelial cells associated with tumor angiogenesis, and Micro-CT imaging has shown a +32 or - 8 HU increase in the signal of the targeted liposomes<sup>50</sup>. Thus, the advances in targeting, widespread availability, and common clinical use make iodine contrast agent attractive candidates for inner ear imaging.

**Gold Compounds**—When gold is used as a contrast agent it is normally in the form of nanoparticles<sup>51</sup>. These particles possess a range of physical and chemical properties that are

important in CT contrast agents. The contrast enhancement of these nanoparticles is consistent regardless of nanoparticle size or shape<sup>52</sup>. Gold nanoparticles' retention times are much higher than the iodine contrast agents and PEG-modified gold nanoparticles have been shown to exhibit a long circulation time within the body<sup>53</sup>. As a noble metal, gold is highly biocompatible and possesses low cytotoxicity<sup>54</sup>. Significantly, under most conditions, gold's ability to absorb x-rays is greater than iodine's, with gold being able to produce 2.7 times greater contrast per unit of mass than iodine when scanned at 120keV<sup>55</sup>.

Gold nanoparticles have been used in several clinical trials and have demonstrated all of the safe features<sup>56</sup>. One of the major reasons for the interest is the ease at which the particles can be conjugated to targeting agents using NHS/EDC chemistry<sup>57</sup>. The use of targeted gold nanoparticles to visualize head and neck cancer cells produced an approximately 5 fold higher x-ray absorption<sup>57</sup> and a several fold increase on prostate cancer cells<sup>58</sup> compared to non-targeted gold agents. Another group was able to visualize tumors as small as 4 mm using targeted agents<sup>59</sup>. Finally, targeted gold nanoparticles were successfully used to visualize cerebral thromboemboli<sup>60</sup>.

Gold nanoparticles possess great potential for inner ear imaging, as they are non-toxic, highly unreactive and can produce strong signal enhancement in CT scans. However, the major advantage of using gold nanoparticles is the ease with which they can be targeted. Gold nanoparticles are widely used in the synthesis of targeted CT contrast agents and can enable the visualization of small structures. This is critical for imaging of the inner ear given the size of its components. Thus, targeted gold agents have the potential to fill a niche in CT imaging where they could be used clinically to target specific proteins such as tumor biomarkers.

**Bismuth**—Bismuth sulfide nanoparticles are cost efficient contrast agents with many desirable physical and chemical properties<sup>61, 62</sup>. These nanoparticles are able to produce five times higher X-ray absorption and are cleared from the body at a much slower rate than iodine contrast agents<sup>63</sup>. Like many other contrast agents, significant levels of cytotoxicity are observed when using a simple bismuth salt<sup>63</sup>. This has led to the development of coated bismuth nanoparticles<sup>61, 63, 64</sup>. Oleate-coated bismuth sulfide nanoparticles that target breast cancer cells have been manufactured<sup>64</sup>. The use of these targeted nanoparticles was shown by micro-CT analysis to produce a 1.6 times greater accumulation of the particles in the tumor compared to when untargeted particles were used<sup>64</sup>. Targeted nanoparticles also improved the visualization of the tumor boundaries and showed minimal cytotoxicity<sup>64</sup>. Bismuth nanoparticles may prove to be suitable targeted contrast agents for inner ear imaging, but more data are required.

## Imaging of the inner ear

The modality used to image the inner ear currently depends on the structures to be imaged. CT is widely used to image the osseous structures<sup>4</sup> while MRI is used to image the fluid compartments<sup>65</sup> (Table 1). Untargeted gadolinium contrast agents are capable of passing through the blood labyrinth barrier and intravenous delivery of these agents is a common means of administration<sup>18, 19</sup>. However, local administration may be able to increase the

targeting efficiency of a given contrast agent. Some success has been achieved delivering gadolinium contrast agents locally to the inner ear by administering the compounds transtympanically<sup>66</sup>, resulting in improved signal to noise ratios in MR imaging. However, some of the best MRI images have been achieved when absorbable gelatin sponges were soaked in a gadolinium contrast agent and placed onto the round window niche allowing the agent to diffuse through the round window into the cochlea<sup>67</sup>. Despite the challenges of inner ear imaging, MRI using gadolinium contrast agents administered by both the intratympanic and intravenous route have facilitated detection of endolymphatic hydrops in patients with Meniere's Disease<sup>18, 65</sup>. Additionally, contrast agent administration via the intrathecal route has enabled the detection of perilymphatic fistula<sup>68</sup> and MRI was able to detect inner ear changes due to inner ear hemorrhage<sup>69</sup>. However, none of them can detect abnormalities at cellular or molecular level. Attempts have been made to use iron oxide in the form of SPION micelles as an inner ear contrast agent. Unfortunately, Poe et al.<sup>70</sup> encountered difficulties diffusing the micelles through the round window membranes of rats. Fortunately, Ge et al.<sup>71</sup> were able to pass large amounts of SPION nanoparticles through the round window membrane of chinchillas. However, Ge et al. used histological techniques and not MRI to demonstrate that the SPIONs had reached the inner ear. The possibility that the differences in SPION diffusion are species related cannot be ruled out. However, it appears that the major difference between the two sets of SPIONs was the material used to coat the nanoparticles<sup>70, 71</sup>. Optimization of the SPION coating will hopefully allow for efficient diffusion SPION micelles through the round window membrane making imaging of this type routine.

Regrettably, at this point the ability of targeted gold to diffuse through the round window membrane and enhance CT imaging is unknown. However, although Iodine based contrast agents are also not able to pass through middle-inner ear barriers or the blood-inner ear barriers Iodine based agents have been used to visualize cochlear soft tissue *ex vivo*<sup>72</sup>. Significantly, gold nanoparticles have the advantage over iodine agents as they are non-toxic<sup>54</sup>, are easy to conjugate<sup>57</sup> and produce higher levels of CT contrast at 120keV<sup>51</sup>. The development targeted CT contrast agents should enhance the cochlear soft tissue imaging. This development complements CT's detailed imaging of the temporal bone and should meet physicians' diagnostic needs for potential cell and molecular therapy.

## Conclusion

Currently, many of the underlying causes of hearing loss, including hair cell loss, are undetectable by current clinical MR or CT<sup>2,5</sup>. The use of targeted contrast agents will be required to enable either modality to detect the microscopic structural changes, or even molecular abnormalities, underlying this loss. The targeting agent employed will vary depending on the suspected cause of hearing loss. For instance, nanoparticles conjugated to prestin binding peptides<sup>73</sup> could be delivered to the cochlea in order to measure the loss of outer hair cells.

Alternatively, if damage to the cochlear nerve is suspected, nanoparticles conjugated to the Tet 1 peptide<sup>74</sup> could be used to determine nerve damage. In addition to peptides, contrast

agents can be conjugated to antibodies, allowing the agents to bind specifically to inner ear biomarkers such as Myosin VIIa<sup>75</sup>.

The ideal targeted contrast agent for inner ear imaging will be one that is non-toxic, passes through the 1 micron pores of the round window membrane<sup>76</sup>, or at least is able to pass through the labyrinth blood barrier (Figure 1), produces a high degree of contrast enhancement, and is easy to conjugate. Unfortunately, no current contrast agent fulfills all of these criteria. Gadolinium compounds can diffuse through the round window membrane(Figure 2, 4)<sup>67</sup> and produce a high degree of MRI contrast enhancement<sup>22</sup>. However, these compounds are difficult to conjugate<sup>22</sup> and they have potential toxicity<sup>27</sup>. Meanwhile SPION constructs are easy to conjugate,<sup>42</sup> and exhibit minimal cytotoxicity<sup>44</sup>. Unfortunately, the negative contrast produced by the SPIONs makes them less desirable clinically, and their ability to pass through the round window membrane still has to be optimized<sup>70</sup>. Despite their drawbacks, MRI contrast agents are currently more useful<sup>18, 19, 65</sup> than CT agents. Although targeted MRI contrast agents can be developed, the temporal bone will still be difficult to visualize using this modality. A potential solution to the difficulties encountered in inner ear molecular imaging would be superimpose the standard CT scan of the inner ear on top of optical imaging obtained using a fluorescent targeted contrast agent. This would allow both the targeted features and the landmarks of the cochlea to be identified<sup>4, 9, 77</sup>.

It is to be hoped that pre-clinical imaging technology such as micro CT<sup>78-80</sup>, which enables the microscopic high resolution imaging of fine structures (Figure 3,4), and improved spectral CT<sup>81, 82</sup> which enables subtle changes in contrast to be easily visualized, will lead to increased sensitivity of CT inner ear imaging. In addition, middle ear structures have been detected by ultrasound, so with the use of 3D printing; ultrasound may have a role in inner ear imaging<sup>83</sup>. It is also clear that the diffusion characteristics of the agents through round window membrane<sup>70</sup> will need to be optimized before they can routinely be applied locally. Improvements in imaging technology together with the development of targeted inner ear contrast agents may enable molecular and morphological alterations within the inner ear to be detected. This ability fulfills a clinical need and could revolutionize the diagnosis and treatment of diseases of the inner ear.

## Acknowledgments

This work was funded through a National Institute of Health (NIH) grant: 1R01DC014464-01.

## References

1. Lin FR, Niparko JK, Ferrucci L. Hearing loss prevalence in the United States. *Arch Intern Med.* Nov 14; 2011 171(20):1851–1852. [PubMed: 22083573]
2. Dror AA, Avraham KB. Hearing loss: mechanisms revealed by genetics and cell biology. *Annu Rev Genet.* 2009; 43:411–437. [PubMed: 19694516]
3. Shearer, AE., Hildebrand, MS., Smith, RJH. Deafness and Hereditary Hearing Loss Overview. In: Pagon, RA. Adam, MP. Ardinger, HH. Wallace, SE. Amemiya, A. Bean, LJH., et al., editors. *GeneReviews(R)*. Seattle (WA): 2017.



4. Joshi VM, Navlekar SK, Kishore GR, Reddy KJ, Kumar EC. CT and MR imaging of the inner ear and brain in children with congenital sensorineural hearing loss. *Radiographics*. May-Jun;2012 32(3):683–698. [PubMed: 22582354]
5. Henderson D, Bielefeld EC, Harris KC, Hu BH. The role of oxidative stress in noise-induced hearing loss. *Ear Hear*. Feb; 2006 27(1):1–19. [PubMed: 16446561]
6. Mathur P, Yang J. Usher syndrome: Hearing loss, retinal degeneration and associated abnormalities. *Biochim Biophys Acta*. Mar; 2015 1852(3):406–420. [PubMed: 25481835]
7. Wathen CA, Foje N, van Avermaete T, Miramontes B, Chapaman SE, Sasser TA, et al. In vivo X-ray computed tomographic imaging of soft tissue with native, intravenous, or oral contrast. *Sensors (Basel)*. 2013; 13(6):6957–6980. [PubMed: 23711461]
8. Giesemann A, Hofmann E. Some Remarks on Imaging of the Inner Ear: Options and Limitations. *Clin Neuroradiol*. 2015; 25(2):197–203.
9. Bartling SH, Peldschus K, Rodt T, Kral F, Matthies H, Kikinis R, et al. Registration and fusion of CT and MRI of the temporal bone. *J Comput Assist Tomogr*. May-Jun;2005 29(3):305–310. [PubMed: 15891495]
10. Piromchai P, Kasemsiri P, Thanawirattananit P, Yimtae K. Congenital Malformations of the Inner Ear: Case Series and Review of the Literature. *J Med Assoc Thai*. 2015; 98(7):S217–224. [PubMed: 26742393]
11. Abele TA, Wiggins RH 3rd. Imaging of the temporal bone. *Radiol Clin North Am*. 2015; 53(1):15–36. [PubMed: 25476172]
12. Marziano NK, Casalotti SO, Portelli AE, Becker DL, Forge A. Mutations in the gene for connexin 26 (GJB2) that cause hearing loss have a dominant negative effect on connexin 30. *Hum Mol Genet*. Apr 15; 2003 12(8):805–812. [PubMed: 12668604]
13. Lohrke J, Frenzel T, Endrikat J, Alves FC, Grist TM, Law M, et al. 25 Years of Contrast-Enhanced MRI: Developments, Current Challenges and Future Perspectives. *Adv Ther*. Jan; 2016 33(1):1–28. [PubMed: 26809251]
14. Lusic H, Grinstaff MW. X-ray-computed tomography contrast agents. *Chem Rev*. Mar 13; 2013 113(3):1641–1666. [PubMed: 23210836]
15. Cormode DP, Naha PC, Fayad ZA. Nanoparticle contrast agents for computed tomography: a focus on micelles. *Contrast Media Mol Imaging*. Jan-Feb;2014 9(1):37–52. [PubMed: 24470293]
16. Pierre VC, Allen MJ, Caravan P. Contrast agents for MRI: 30+ years and where are we going? *J Biol Inorg Chem*. Feb; 2014 19(2):127–131. [PubMed: 24414380]
17. Pakdaman MN, Ishiyama G, Ishiyama A, Peng KA, Kim HJ, Pope WB, et al. Blood-Labyrinth Barrier Permeability in Meniere Disease and Idiopathic Sudden Sensorineural Hearing Loss: Findings on Delayed Postcontrast 3D-FLAIR MRI. *AJNR Am J Neuroradiol*. Jun 2.2016
18. Fukushima M, Oya R, Akazawa H, Tsuruta Y, Inohara H. Gadolinium-enhanced inner ear magnetic resonance imaging for evaluation of delayed endolymphatic hydrops, including a bilateral case. *Acta Otolaryngol*. May; 2016 136(5):451–455. [PubMed: 26799493]
19. Naganawa S, Yamazaki M, Kawai H, Bokura K, Sone M, Nakashima T. Imaging of Meniere's disease after intravenous administration of single-dose gadodiamide: utility of subtraction images with different inversion time. *Magn Reson Med Sci*. 2012; 11(3):213–219. [PubMed: 23037568]
20. Raymond KN, Pierre VC. Next generation, high relaxivity gadolinium MRI agents. *Bioconjug Chem*. Jan-Feb;2005 16(1):3–8. [PubMed: 15656568]
21. Telgmann L, Sperling M, Karst U. Determination of gadolinium-based MRI contrast agents in biological and environmental samples: a review. *Anal Chim Acta*. Feb 18.2013 764:1–16. [PubMed: 23374209]
22. Caravan P, Das B, Dumas S, Epstein FH, Helm PA, Jacques V, et al. Collagen-targeted MRI contrast agent for molecular imaging of fibrosis. *Angew Chem Int Ed Engl*. 2007; 46(43):8171–8173. [PubMed: 17893943]
23. Na JH, Lee S, Koo H, Han H, Lee KE, Han SJ, et al. T1-Weighted MR imaging of liver tumor by gadolinium-encapsulated glycol chitosan nanoparticles without non-specific toxicity in normal tissues. *Nanoscale*. May 5; 2016 8(18):9736–9745. [PubMed: 27113247]

24. Tanifum EA, Ghaghada K, Vollert C, Head E, Eriksen JL, Annapragada A. A Novel Liposomal Nanoparticle for the Imaging of Amyloid Plaque by Magnetic Resonance Imaging. *J Alzheimers Dis.* Mar 25; 2016 52(2):731–745. [PubMed: 27031484]
25. Liu X, Madhankumar AB, Miller PA, Duck KA, Hafenstein S, Rizk E, et al. MRI contrast agent for targeting glioma: interleukin-13 labeled liposome encapsulating gadolinium-DTPA. *Neuro Oncol.* May; 2016 18(5):691–699. [PubMed: 26519740]
26. Kaewlai R, Abujdeh H. Nephrogenic systemic fibrosis. *AJR Am J Roentgenol.* Jul; 2012 199(1):W17–23. [PubMed: 22733927]
27. Kanda T, Fukusato T, Matsuda M, Toyoda K, Oba H, Kotoku J, et al. Gadolinium-based Contrast Agent Accumulates in the Brain Even in Subjects without Severe Renal Dysfunction: Evaluation of Autopsy Brain Specimens with Inductively Coupled Plasma Mass Spectroscopy. *Radiology.* Jul; 2015 276(1):228–232. [PubMed: 25942417]
28. McDonald RJ, McDonald JS, Kallmes DF, Jentoft ME, Murray DL, Thielen KR, et al. Intracranial Gadolinium Deposition after Contrast-enhanced MR Imaging. *Radiology.* Jun; 2015 275(3):772–782. [PubMed: 25742194]
29. Errante Y, Cirimele V, Mallio CA, Di Lazzaro V, Zobel BB, Quattrocchi CC. Progressive increase of T1 signal intensity of the dentate nucleus on unenhanced magnetic resonance images is associated with cumulative doses of intravenously administered gadodiamide in patients with normal renal function, suggesting dechelation. *Invest Radiol.* Oct; 2014 49(10):685–690. [PubMed: 24872007]
30. Reeder SB, Gulani V. Gadolinium Deposition in the Brain: Do We Know Enough to Change Practice? *Radiology.* Apr; 2016 279(1):323–326.
31. Runge VM. Safety of the Gadolinium-Based Contrast Agents for Magnetic Resonance Imaging, Focusing in Part on Their Accumulation in the Brain and Especially the Dentate Nucleus. *Invest Radiol.* May; 2016 51(5):273–279. [PubMed: 26945278]
32. Lin SP, Brown JJ. MR contrast agents: physical and pharmacologic basics. *J Magn Reson Imaging.* May; 2007 25(5):884–899. [PubMed: 17457803]
33. Schabelman E, Witting M. The relationship of radiocontrast, iodine, and seafood allergies: a medical myth exposed. *J Emerg Med.* Nov; 2010 39(5):701–707. [PubMed: 20045605]
34. Jin R, Lin B, Li D, Ai H. Superparamagnetic iron oxide nanoparticles for MR imaging and therapy: design considerations and clinical applications. *Curr Opin Pharmacol.* Oct.2014 18:18–27. [PubMed: 25173782]
35. Shokrollahi H. Structure, synthetic methods, magnetic properties and biomedical applications of ferrofluids. *Mater Sci Eng C Mater Biol Appl.* Jul 1; 2013 33(5):2476–2487. [PubMed: 23623058]
36. Na HB, Song IC, Hyeon T. Inorganic Nanoparticles for MRI Contrast Agents. *Advanced Materials.* 2009; 21:2133–2148.
37. Moteki T, Horikoshi H. Evaluation of Hepatic Lesions and Hepatic Parenchyma Using Diffusion-Weighted Echo-Planar MR With Three Values of Gradient b-Factor. *Journal of Magnetic Resonance Imaging.* 2006; 24:637–645. [PubMed: 16888790]
38. Harisinghani MG, Barentsz J, Hahn PF, Deserno WM, Tabatabaei S, van de Kaa CH, et al. Noninvasive detection of clinically occult lymph-node metastases in prostate cancer. *N Engl J Med.* Jun 19; 2003 348(25):2491–2499. [PubMed: 12815134]
39. Stabi KL, Bendz LM. Ferumoxylol use as an intravenous contrast agent for magnetic resonance angiography. *Ann Pharmacother.* Dec; 2011 45(12):1571–1575. [PubMed: 22045905]
40. Wang YX. Current status of superparamagnetic iron oxide contrast agents for liver magnetic resonance imaging. *World J Gastroenterol.* Dec 21; 2015 21(47):13400–13402. [PubMed: 26715826]
41. Kim YK, Kim CS, Kwak HS, Lee JM. Three-dimensional dynamic liver MR imaging using sensitivity encoding for detection of hepatocellular carcinomas: comparison with superparamagnetic iron oxide-enhanced mr imaging. *J Magn Reson Imaging.* Nov; 2004 20(5): 826–837. [PubMed: 15503325]
42. Xiao Y, Lin ZT, Chen Y, Wang H, Deng YL, Le DE, et al. High molecular weight chitosan derivative polymeric micelles encapsulating superparamagnetic iron oxide for tumor-targeted magnetic resonance imaging. *Int J Nanomedicine.* 2015; 10:1155–1172. [PubMed: 25709439]

43. Sillerud LO, Solberg NO, Chamberlain R, Orlando RA, Heidrich JE, Brown DC, et al. SPION-enhanced magnetic resonance imaging of Alzheimer's disease plaques in AbetaPP/PS-1 transgenic mouse brain. *J Alzheimers Dis.* 2013; 34(2):349–365. [PubMed: 23229079]
44. Mahmoudi M, Simchi A, Milani AS, Stroeve P. Cell toxicity of superparamagnetic iron oxide nanoparticles. *J Colloid Interface Sci.* Aug 15; 2009 336(2):510–518. [PubMed: 19476952]
45. Melhem ER, Shakir H, Bakthavachalam S, MacDonald CB, Gira J, Caruthers SD, et al. Inner ear volumetric measurements using high-resolution 3D T2-weighted fast spin-echo MR imaging: initial experience in healthy subjects. *AJNR Am J Neuroradiol.* Nov-Dec;1998 19(10):1819–1822. [PubMed: 9874529]
46. Kovacsovic B, Davidsson L, Harder H, Magnuson B, Ledin T. MRI screening of the cerebellopontine angle and inner ear with fast spin-echo T2 technique. *Arch Ital Biol.* Jan; 2000 138(1):87–92. [PubMed: 10604036]
47. Chalikias G, Drosos I, Tziakas DN. Contrast-Induced Acute Kidney Injury: An Update. *Cardiovasc Drugs Ther.* Apr; 2016 30(2):215–228. [PubMed: 26780748]
48. Widmark JM. Imaging-related medications: a class overview. *Proc (Bayl Univ Med Cent).* Oct; 2007 20(4):408–417. [PubMed: 17948119]
49. Mukundan S, Ghaghada KB, Badaea CT, Kao CY, Hedlund LW, Provenzale JM, et al. A liposomal nanoscale contrast agent for preclinical CT in mice. *AJR Am J Roentgenol.* Feb; 2006 186(2):300–307. [PubMed: 16423931]
50. Wyss C, Schaefer SC, Juillerat-Jeanneret L, Lagopoulos L, Lehr HA, Becker CD, et al. Molecular imaging by micro-CT: specific E-selectin imaging. *Eur Radiol.* Oct; 2009 19(10):2487–2494. [PubMed: 19440717]
51. Hainfeld JF, Slatkin DN, Focella TM, Smilowitz HM. Gold nanoparticles: a new X-ray contrast agent. *Br J Radiol.* Mar; 2006 79(939):248–253. [PubMed: 16498039]
52. Jackson P, Periasamy S, Bansal V, Geso M. Evaluation of the effects of gold nanoparticle shape and size on contrast enhancement in radiological imaging. *Australas Phys Eng Sci Med.* 2011; 34(2):243–249. [PubMed: 21465276]
53. Niidome T, Yamagata M, Okamoto Y, Akiyama Y, Takahashi H, Kawano T, et al. PEG-modified gold nanorods with a stealth character for in vivo applications. *J Control Release.* Sep 12; 2006 114(3):343–347. [PubMed: 16876898]
54. Fratoddi I, Venditti I, Cametti C, Russo MV. How toxic are gold nanoparticles? The state-of-the-art. *Nano Res.* Jun; 2015 8(6):1771–1799.
55. <http://physics.nist.gov/PhysRefData/XrayMassCoef>
56. Anselmo AC, Mitragotri S. Nanoparticles in the clinic. *BioengTransl Med.* 2016; 1(1):10–29.
57. Popovtzer R, Agrawal A, Kotov NA, Popovtzer A, Balter J, Carey TE, et al. Targeted gold nanoparticles enable molecular CT imaging of cancer. *Nano Lett.* Dec; 2008 8(12):4593–4596. [PubMed: 19367807]
58. Chanda N, Kattumuri V, Shukla R, Zambre A, Katti K, Upendran A, et al. Bombesin functionalized gold nanoparticles show in vitro and in vivo cancer receptor specificity. *Proc Natl Acad Sci U S A.* May 11; 2010 107(19):8760–8765. [PubMed: 20410458]
59. Reuveni T, Motiei M, Romman Z, Popovtzer A, Popovtzer R. Targeted gold nanoparticles enable molecular CT imaging of cancer: an in vivo study. *Int J Nanomedicine.* 2011; 6:2859–2864. [PubMed: 22131831]
60. Kim JY, Ryu JH, Schellingerhout D, Sun IC, Lee SK, Jeon S, et al. Direct Imaging of Cerebral Thromboemboli Using Computed Tomography and Fibrin-targeted Gold Nanoparticles. *Theranostics.* 2015; 5(10):1098–1114. [PubMed: 26199648]
61. Wei B, Zhang X, Zhang C, Jiang Y, Fu YY, Yu C, et al. Facile Synthesis of Uniform-Sized Bismuth Nanoparticles for CT Visualization of Gastrointestinal Tract in Vivo. *ACS Appl Mater Interfaces.* May 25; 2016 8(20):12720–12726. [PubMed: 27144639]
62. Brown AL, Naha PC, Benavides-Montes V, Litt HI, Goforth AM, Cormode DP. Synthesis, X-ray Opacity, and Biological Compatibility of Ultra-High Payload Elemental Bismuth Nanoparticle X-ray Contrast Agents. *Chem Mater.* Apr 8; 2014 26(7):2266–2274. [PubMed: 24803727]

63. Rabin O, Manuel Perez J, Grimm J, Wojtkiewicz G, Weissleder R. An X-ray computed tomography imaging agent based on long-circulating bismuth sulphide nanoparticles. *Nat Mater*. Feb; 2006 5(2):118–122. [PubMed: 16444262]
64. Kinsella JM, Jimenez RE, Karmali PP, Rush AM, Kotamraju VR, Gianneschi NC, et al. X-ray computed tomography imaging of breast cancer by using targeted peptide-labeled bismuth sulfide nanoparticles. *Angew Chem Int Ed Engl*. Dec 16; 2011 50(51):12308–12311. [PubMed: 22028313]
65. Pyykko I, Zou J, Poe D, Nakashima T, Naganawa S. Magnetic resonance imaging of the inner ear in Meniere's disease. *Otolaryngol Clin North Am*. Oct; 2010 43(5):1059–1080. [PubMed: 20713245]
66. Zou J, Poe D, Bjelke B, Pyykko I. Visualization of inner ear disorders with MRI in vivo: from animal models to human application. *Acta Otolaryngol Suppl*. Feb.2009 (560):22–31. [PubMed: 19221903]
67. Zou J, Zhang W, Poe D, Zhang Y, Ramadan UA, Pyykko I. Differential passage of gadolinium through the mouse inner ear barriers evaluated with 4.7T MRI. *Hear Res*. Jan; 2010 259(1-2):36–43. [PubMed: 19818391]
68. Morris MS, Kil J, Carvlin MJ. Magnetic resonance imaging of perilymphatic fistula. *The Laryngoscope*. 1993; 103(7):729–733. [PubMed: 8341096]
69. Wu X, Chen K, Sun L, Yang Z, Zhu Y, Jiang H. Magnetic resonance imaging-detected inner ear hemorrhage as a potential cause of sudden sensorineural hearing loss. *Am J Otolaryngol*. 2014; 35(3):318–323. [PubMed: 24629585]
70. Poe D, Zou J, Bjelke B, Pyykkö I. MRI of the Cochlea with Superparamagnetic iron oxide nanoparticles compared to Gadolinium chelate contrast agents in a rat model *European Journal of Nanomedicine*. 2009; 2(2):29–36.
71. Ge X, Jackson RL, Liu J, Harper EA, Hoffer ME, Wassel RA, et al. Distribution of PLGA nanoparticles in chinchilla cochleae. *Otolaryngol Head Neck Surg*. Oct; 2007 137(4):619–623. [PubMed: 17903580]
72. Zou J, Hannula M, Misra S, Feng H, Labrador RH, Aula AS, et al. Micro CT visualization of silver nanoparticles in the middle and inner ear of rat and transportation pathway after transtympanic injection. *J Nanobiotechnology*. 2015; 13:5. [PubMed: 25622551]
73. Surovtseva EV, Johnston AH, Zhang W, Zhang Y, Kim A, Murakoshi M, et al. Prestin binding peptides as ligands for targeted polymersome mediated drug delivery to outer hair cells in the inner ear. *Int J Pharm*. Mar 15; 2012 424(1-2):121–127. [PubMed: 22227343]
74. Zhang Y, Zhang W, Johnston AH, Newman TA, Pyykko I, Zou J. Targeted delivery of Tet1 peptide functionalized polymersomes to the rat cochlear nerve. *Int J Nanomedicine*. 2012; 7:1015–1022. [PubMed: 22403485]
75. Weil D, Levy G, Sahly I, Levi-Acobas F, Blanchard S, El-Amraoui A, et al. Human myosin VIIA responsible for the Usher 1B syndrome: a predicted membrane-associated motor protein expressed in developing sensory epithelia. *P Natl Acad Sci USA*. 1996; 93(8):3232–3237.
76. Goycoolea MV, Lundman L. Round window membrane. Structure function and permeability: a review. *Microsc Res Tech*. 1997; 36(3):201–211. [PubMed: 9080410]
77. Westerhof JP, Rademaker J, Weber BP, Becker H. Congenital malformations of the inner ear and the vestibulocochlear nerve in children with sensorineural hearing loss: evaluation with CT and MRI. *J Comput Assist Tomogr*. Sep-Oct;2001 25(5):719–726. [PubMed: 11584231]
78. Wintermark M, Jawadi SS, Rapp JH, Tihan T, Tong E, Glidden DV, et al. High-resolution CT imaging of carotid artery atherosclerotic plaques. *AJNR Am J Neuroradiol*. May; 2008 29(5):875–882. [PubMed: 18272562]
79. Ritman EL. Current status of developments and applications of micro-CT. *Annu Rev Biomed Eng*. Aug 15.2011 13:531–552. [PubMed: 21756145]
80. Ashton JR, West JL, Badea CT. In vivo small animal micro-CT using nanoparticle contrast agents. *Front Pharmacol*. 2015; 6:256. [PubMed: 26581654]
81. Silva AC, Morse BG, Hara AK, Paden RG, Hongo N, Pavlicek W. Dual-energy (spectral) CT: applications in abdominal imaging. *Radiographics*. Jul-Aug;2011 31(4):1031–1046. discussion 1047-1050. [PubMed: 21768237]

82. Danad I, Fayad ZA, Willemink MJ, Min JK. New Applications of Cardiac Computed Tomography: Dual-Energy, Spectral, and Molecular CT Imaging. *JACC Cardiovasc Imaging*. Jun; 2015 8(6): 710–723. [PubMed: 26068288]
83. Brown JA, Torbatian Z, Adamson RB, Van Wijhe R, Pennings RJ, Lockwood GR, et al. High-frequency ex vivo ultrasound imaging of the auditory system. *Ultrasound Med Biol*. 2009; 35(11): 1899–1907. [PubMed: 19679390]

## Abbreviations

<b>SPIONs</b>	Superparamagnetic iron oxide nanoparticles
<b>USPION</b>	Ultra small superparamagnetic iron oxide nanoparticles
<b>NHS</b>	N-Hydroxysuccinimide
<b>EDC</b>	Ethyl(dimethylaminopropyl) carbodiimide
<b>MTT</b>	3-(4,5-Dimethylthiazol-2-Yl)-2,5-diphenyltetrazolium bromide

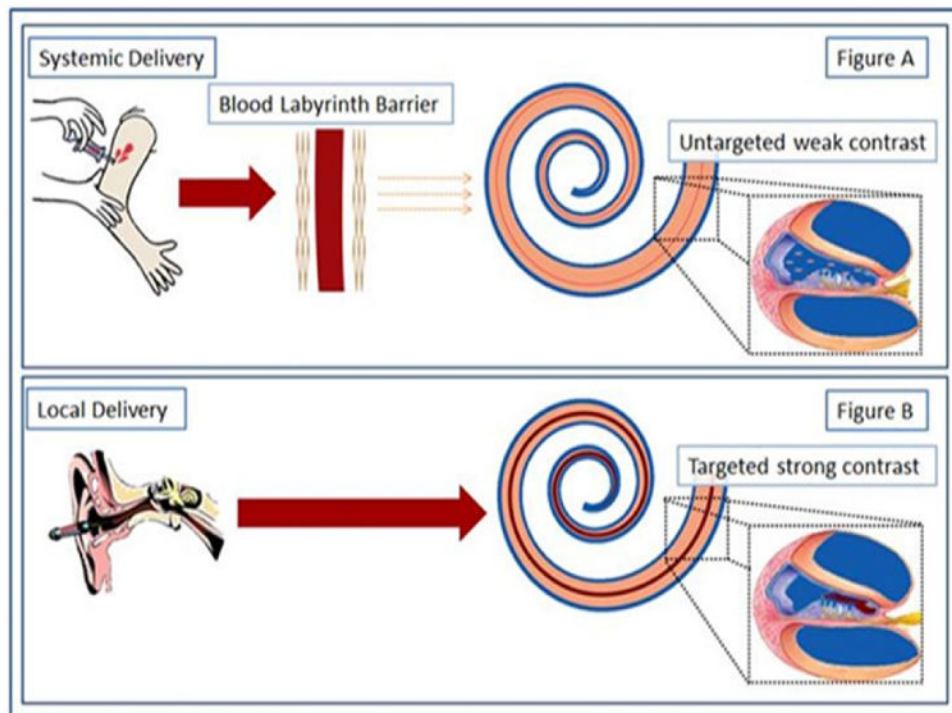


**Figure 1. Contrast Agent delivery to the inner ear**

There are two routes available for the delivery of contrast agents. (Figure A) Systemic delivery is inefficient with the distribution problems being exacerbated by the blood labyrinth barrier. This can impede contrast agent delivery and may result in insufficient amounts of the agent reaching the inner ear. Transtympanic, (Figure B) local delivery efficiently delivers the contrast agent into the cochlea.

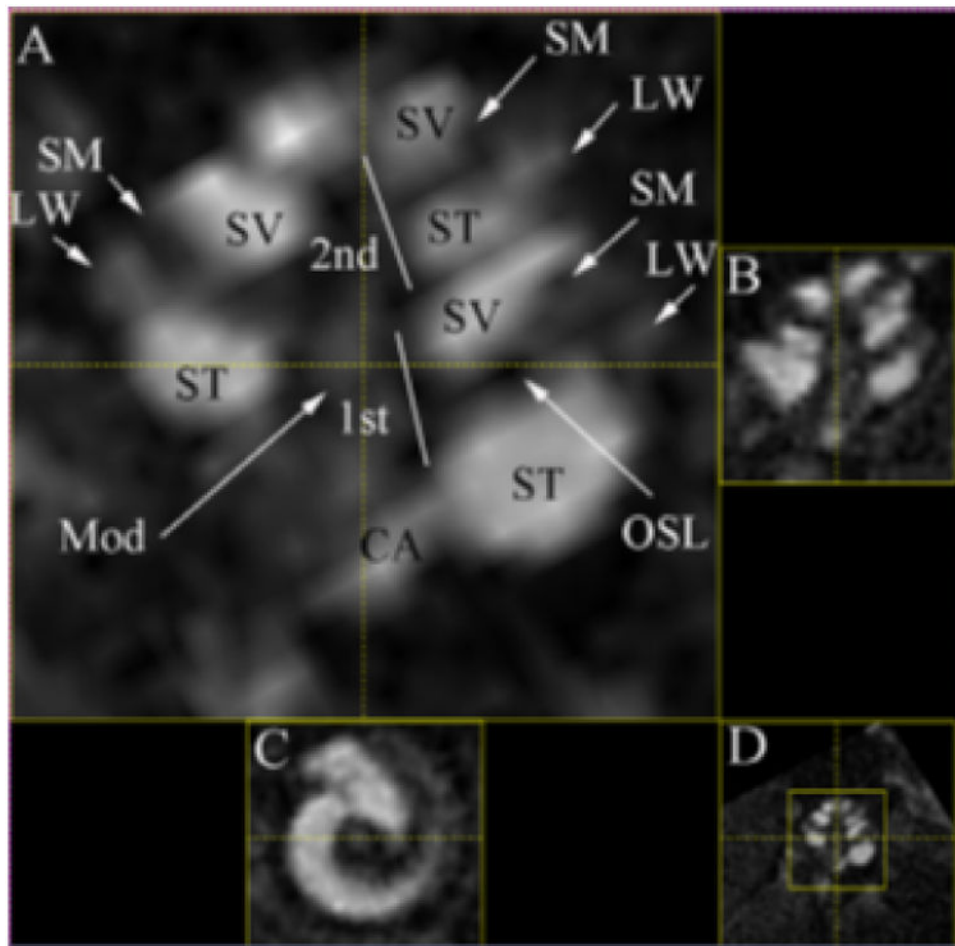


**Figure 2. Enhancement mouse cochlea MR image using a Gadolinium contrast agent**  
 Mouse cochlear structures in MPR multi view of T1-weighted images with IT administration of Gd-DOTA (23 mm coil) (180 min time point). Gelfoam soaked with 5  $\mu$ L, 500 mmol/L Gd-DOTA was placed into the left ear. In the enlarged window A, LW and Mod are slightly highlighted by Gd-DOTA uptake in addition to more pronounced enhancement in ST and SV. The structure adjacent to ST is suspected to be CA with signal intensity similar to ST. LW demonstrated brighter signal than SM. A dark border appeared between ST and LW in the basal turn near the hook region. OSL is seen as a sharp dark line. Small window B is a relative perpendicular cut through the center of plane A. Small window C is a relative axial cut through the center of the cochlea in window A. Small window D is the minimized image of window A. CA, cochlear aqueduct; LW, lateral wall; Mod, modiolus; MPR, multiplanar reconstruction; OSL, osseous spiral lamina; SM, the scala media; ST, the scala tympani; SV, the scala vestibuli; 1st, the basal turn; 2nd, the second turn. Reprinted from Zou et al (2010)<sup>67</sup>.

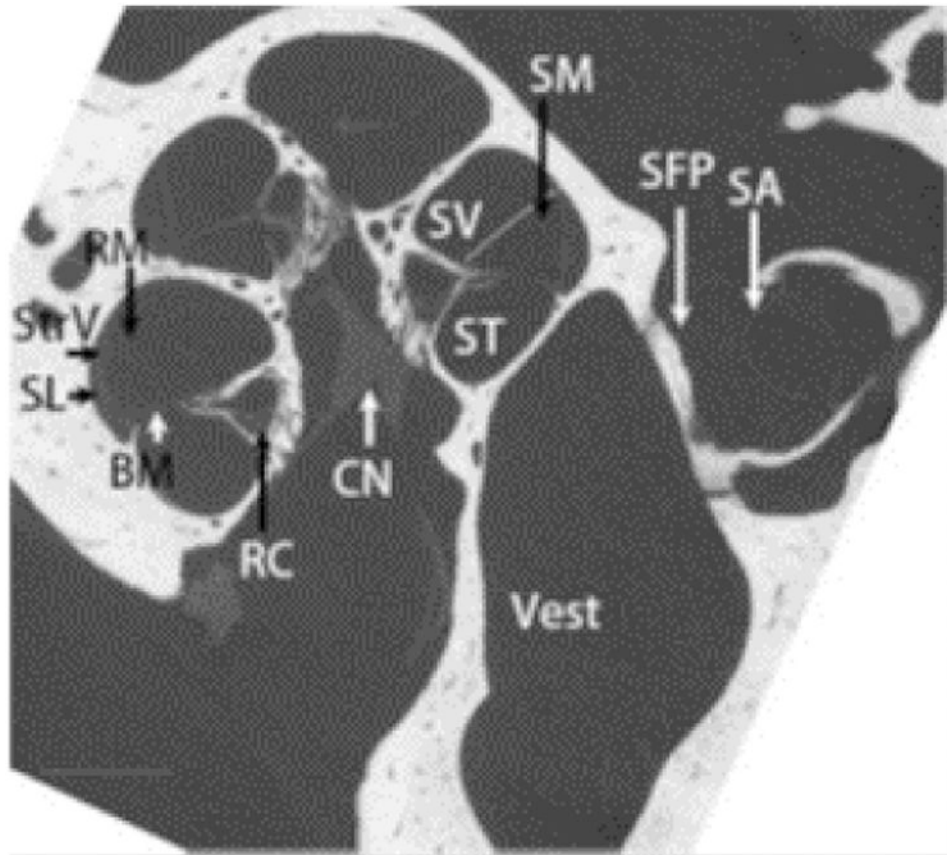


**Figure 3. Enhancement of the Rat cochlea CT image using an Iodine contrast agent**

The heterogeneous fine structures of rat inner ear were demonstrated using iodine-contrasted micro CT (BM: basilar membrane; CN: cochlear nerve; RM: Reissner's membrane; SA: stapedial artery; SFP: stapes footplate; ST: scala tympani; SV: scala vestibuli; Vest: vestibule.) scale bar = 500  $\mu$ m. Reprinted from Zou et al (2015)<sup>72</sup>.



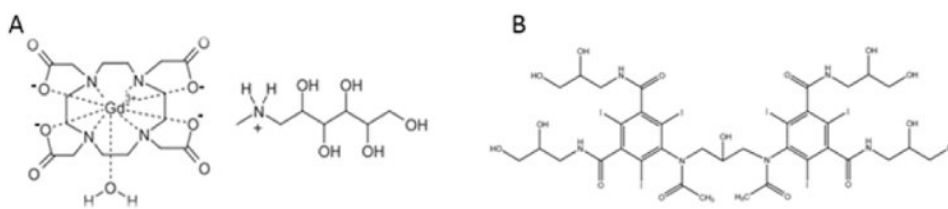


**Figure 4. The chemical structure of two commonly used contrast agents**

(A) The chemical structure of DOTAREM (gadoterate meglumine) (Guerbet, Aulnay-sous-Bois, France), the Gadolinium contrast agent used in the MRI study shown in Figure 2. (B) The chemical structure of VISIPAQUE (iodixanol) (GE Healthcare, Helsinki, Finland), the Iodine based contrast agent used in the CT scan Image illustrated in Figure 3.

**Table 1**

**Comparison between CT scan and MR imaging**

Imaging modality	Able to detect landmarks	Able to detect soft tissue	Sensitivity		Contrast agents		Targeting		
			Able to detect landmarks	Able to detect soft tissue	Systemic delivery	Local delivery	Systemic delivery	Local delivery	Systemic delivery
CT scan	+++	-	+	-	+++	+/-	+/+	+/+	+/+
MRI	+	+++	+++	+++	+++	+/+	+++	+++	+++